# Original Paper —

# Possible kilometer-scale hydrothermal circulation within the Iheya-North field, mid-Okinawa Trough, as inferred from heat flow data

Yuka Masaki<sup>1,2\*</sup>, Masataka Kinoshita<sup>2\*</sup>, Fumio Inagaki<sup>3</sup>, Satoshi Nakagawa<sup>4</sup>, and Ken Takai<sup>5</sup>

We obtained 78 heat flow measurements during 2002-2008 in the area of the Iheya-North hydrothermal field in the middle Okinawa Trough, in order to clarify the spatial extent of the hydrothermal circulation system. Within a small basin surrounded by knolls, three distinct zones are identified with different heat flow values, which we termed the high-, moderate-, and low-heat-flow zones. In the high-heat-flow zone located near the western edge of the basin, extremely high and widely scattered heat flow values (0.01-100 Wm²) were measured within ~500 m of the active hydrothermal mounds, venting black smoker fluid of maximum 311 °C. With increasing distance east of the high-heat-flow zone, heat flow gradually decreases from 1.0 to ~0.1 Wm² in a region where surface sediment is dominated by clay and a high-resolution bathymetry indicates a smooth seafloor surface. We term this area the moderate-heat-flow zone. Further to the east (~2 km from the high-heat-flow zone), the seafloor consists of coarser sediment with a rugged surface, and heat flow is very low (<0.1 Wm²), as designated the low-heat-flow zone. We suggest that such anomalously low heat flow can be explained by the recharge of seawater into the formation, and that hydrothermal vents or diffuse flow in the high-heat-flow zone can drive this kilometer-scale hydrothermal circulation within the Iheya-North knoll complex, if the sediment below the moderate-heat-flow zone is impermeable enough to prevent vertical fluid migration but is permeable enough to encourage horizontal flow. Although some geological data such as piston core samples, surface morphology and seismic data would support this inference, this hypothesis needs to be tested through more direct evidence and by numerical simulation studies.

Keywords: Iheya-North, hydrothermal circulation, Okinawa Trough, back-arc, heat flow

Received 17 September 2010; Accepted 18 October 2010

- 1 Department of Applied Science, Kochi University
- 2 Institute for Research on Earth Evolution (IFREE), Japan Agency for Marine-Earth Science and Technology (JAMSTEC)
- 3 Kochi Institute for Core Sample Research, Japan Agency for Marine-Earth Science and Technology (JAMSTEC)
- 4 Faculty of Fisheries Sciences, Hokkaido University
- 5 Institute of Biogeosciences (Biogeos), Japan Agency for Marine-Earth Science and Technology (JAMSTEC)

#### \*Corresponding author:

Yuka Masaki

Department of Applied Science, Kochi University 2-5-1 Akebono-cho, Kochi 780-8520, Japan

Institute for Research on Earth Evolution (IFREE),
Japan Agency for Marine-Earth Science and Technology (JAMSTEC)
2-15 Natsushima-cho, Yokosuka 237-0061, Japan
Tel. +81-46-867-9323

Tel. +81-46-867-9323 yuka5n@jamstec.go.jp

Copyright by Japan Agency for Marine-Earth Science and Technology

Masataka Kinoshita

Institute for Research on Earth Evolution (IFREE), Japan Agency for Marine-Earth Science and Technology (JAMSTEC)

2-15 Natsushima-cho, Yokosuka 237-0061, Japan

Tel. +81-46-867-9323 masa@jamstec.go.jp

#### 1. Introduction

Hydrothermal circulation beneath the seafloor is a major process of heat and material exchange between seawater and solid earth. Since hydrothermal circulation is induced by magmatic intrusion beneath the seafloor, it is mostly distributed along the mid-oceanic ridges or active back-arc basins. Hydrothermal activities in back-arc basins have been identified in the Mariana Trough (Craig et al., 1987), Manus Basin (Both et al., 1986), North Fiji Basin (Auzende et al., 1990), and mid-Okinawa Trough (Halbach et al., 1989).

The Okinawa Trough is a back-arc basin of the Ryukyu arc-trench system, and is considered to represent rifting within continental crust. Geophysical, geochemical, and microbiological surveys have been carried out in the trough since the 1980s, with the aim of understanding tectonic,

stratigraphic, and volcanic processes. To date, many hydrothermal sites have been discovered (e.g., Katsura et al., 1986; Kimura et al., 1987; Sibuet et al., 1987). Hydrothermal activity is interpreted to have started after rifting-hosted volcanic activities, of which Iheya-North knoll complex is a typical example (Momma et al., 1996).

Detailed heat flow measurements have been carried out in the Okinawa Trough since 1986 (e.g., Yamano et al., 1986a, 1986b, 1988). High heat flow anomalies are generally observed within ~10 km of the trough axis (Kinoshita et al., 1991). The occurrence of hydrothermal circulation, distributed along the axis, is expected from the wide range of heat flow value, with the highest value exceeding 10 Wm<sup>-2</sup>.

High and scattered heat flow values (0.6-0.7 Wm<sup>-2</sup>) were observed in the axial basins of the Iheya Deep (Fig. 1a) in the mid-Okinawa Trough (Kinoshita, 1995; Yamano et al.,

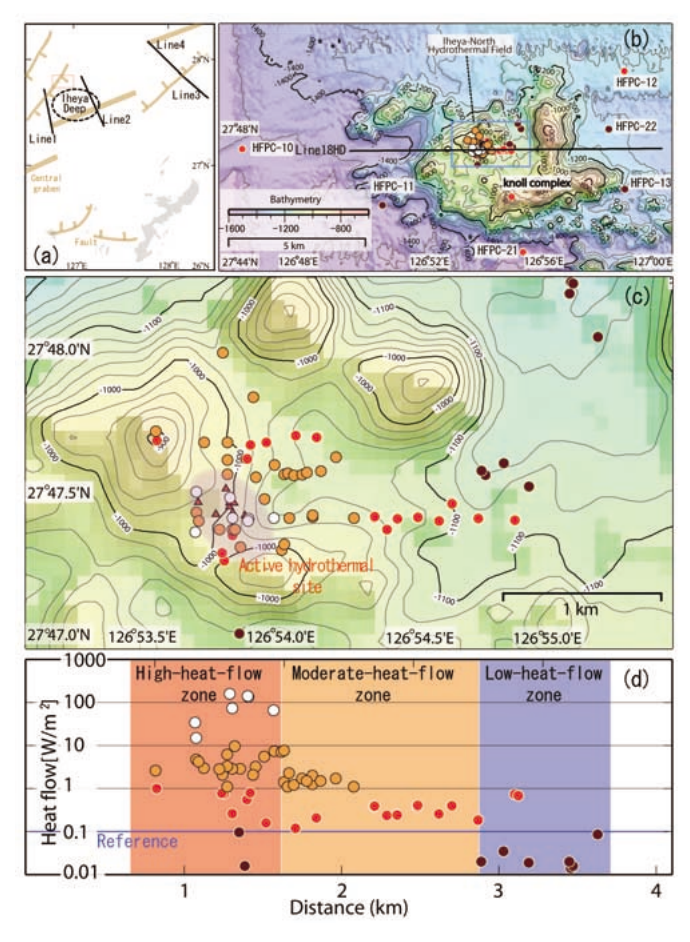


Fig. 1. Bathymetry and heat flow distribution in the Iheya-North hydrothermal field. (a) Index map in the middle Okinawa Trough. Red rectangle shows the location of Iheya-North hydrothermal field. Geological structures are after Kimura et al. (1987). Lines 1-4 in the inset map show the seismic lines surveyed by Nagumo et al. (1986). (b) Bathymetry around the Iheya-North hydrothermal field. Line 18HD: Track line of single channel survey shown in Fig. 5. Blue rectangle represents the area shown in (c). Dots indicates location of heat flow and piston core sampling locations. (c) Bathymetry and heat flow within the Iheya-North hydrothermal field. The color variation of topography is the same scale as in (b). Colored circles show locations of heat flow observations. Heat flow values are color-coded as; white, >10 Wm<sup>-2</sup>; red, 1-10 Wm<sup>-2</sup>; orange, 0.1-1.0 Wm<sup>-2</sup>; and brown, <0.1 Wm<sup>-2</sup>. Red triangles show the locations of hydrothermal mounds in the active hydrothermal site (purple-shaded area). (d) E-W cross-section of heat flow values. Blue line shows the average heat flow value outside the Iheya-North knoll complex.

1986a, 1986b). A seismic reflector at ~1.5 sec (two-way travel time) beneath this site is considered to represent a magma chamber (Nagumo et al., 1986). Kinoshita (1995) conducted a numerical simulation of hydrothermal circulation in this region, assuming magma emplaced at 1.5-2.0 km below the active hydrothermal mound and a basin above the mound covered with impermeable sediment. The simulation results indicated that some seawater is entrained through the basin sediment, as also suggested by concave temperature-depth profiles (Kinoshita et al., 1990), and that heat flow is still high in such a setting because the shallow magma heats the basin by thermal conduction. Thus, the location of the heat source and the permeability structure control the hydrological and thermal regimes in hydrothermal systems.

The Iheya-North hydrothermal field is located northwest of the Iheya-Deep site, 200 km northwest of Okinawa Island (Fig. 1a). The active hydrothermal site, shown as purple region in Fig 1c, is near the western edge of a small basin (~2 km and ~0.7 km in the EW and NS directions, respectively) surrounded by a complex of small knolls. The

hydrothermal edifices are characterized by silty to coarsegrained pumice sand, and by several hydrothermal mounds that produce hydrothermal emissions and that host biological communities (Fig. 2). The most active mound, called the North Big Chimney (NBC), is over 10 m high, and the temperature of venting fluid is 311  $^{\circ}$ C (Kataoka et al., 2000).

Detailed heat flow measurements were performed to understand the spatial extent of the hydrothermal circulation system. Because the characteristics of hydrothermal activity can vary at a local scale, even over distances of less than 1 m, pin-point sampling or measurement with visual confirmation of the site is essential. Given this requirement, investigation using a submersible or Remotely Operated Vehicle (ROV) is most appropriate. In this paper, we present heat flow data collected in and around the Iheya-North hydrothermal field, and propose a qualitative model of hydrothermal circulation inferred from high-resolution bathymetry, side-scan sonar images, core samples, and seismic reflection profiles, as well as heat flow data.

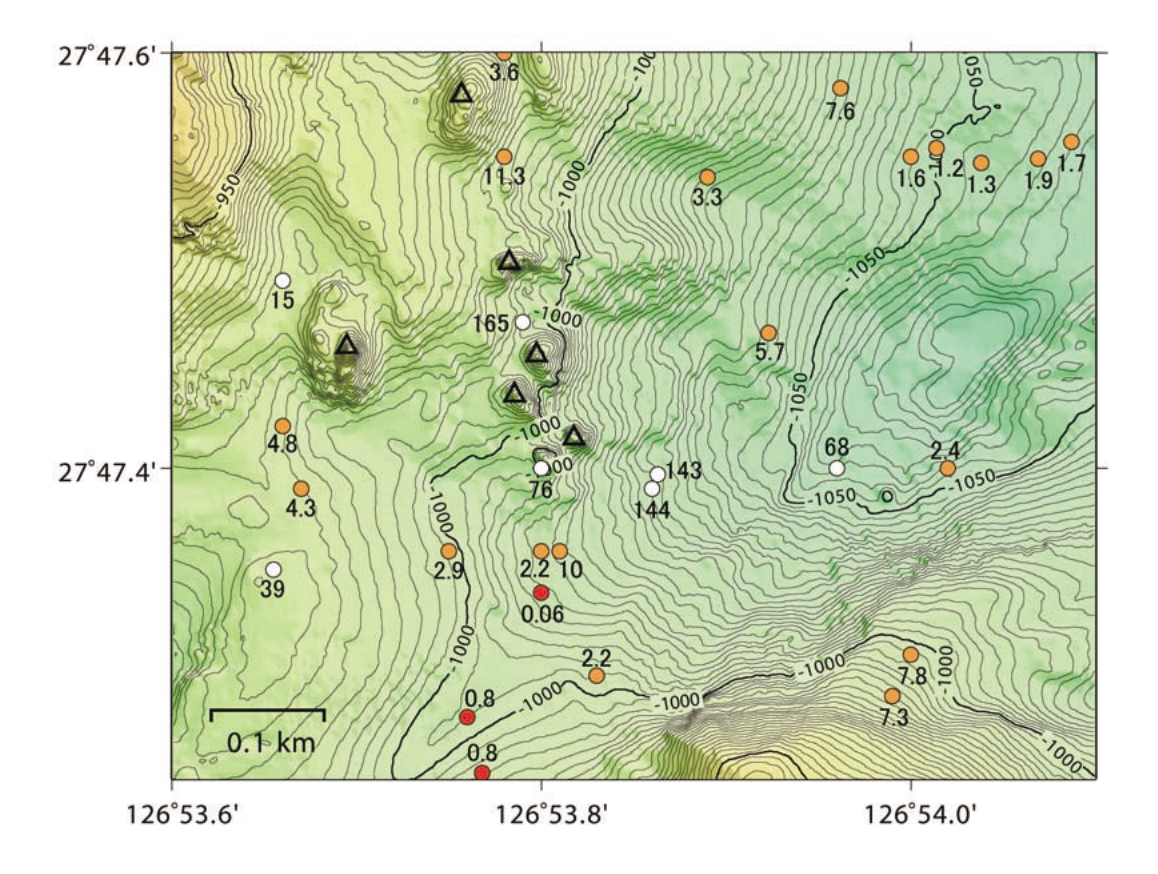


Fig. 2. Heat flow distribution in the high-heat-flow zone (see Fig. 1) of the Iheya-North hydrothermal field. Active hydrothermal mouds are indicated by open triangles. Bathymetry data was obtained by using mult-narrow beam sonar of AUV Urashima (Kumagai et al., 2010); contours are drawn at every 2 m interval. Heat flow stations are shown as filled circles with color codes similar to that in Fig. 1, and the heat flow values are attached with their unit in Wm<sup>-2</sup>.

# 2. Methods

Heat flow measurements were carried out during eight research cruises (NT02-06, NT03-09, KY05-14, YK06-09, YK07-07, NT07-11, NT07-13, and KY08-01) around the Iheya-North hydrothermal field. In 2002-2003, measurements along E-W and N-S transects across the hydrothermal area were performed using the ROV *Hyper Dolphin* of JAMSTEC during the NT02-06 and NT03-09 cruises (Kinoshita et al., 2006a). In 2005, the KY05-14 cruise was undertaken using the Navigable Sampling System (NSS) of the Ocean Research Institute, University of Tokyo, Japan (Kinoshita et al., 2006a). NSS is equipped with thrusters and a TV camera and is capable of operating a piston core sampler or a heat flow probe on the seafloor.

During the YK06-09 cruise in 2006, heat flow measurements were made using the manned research submersible *Shinkai* 6500 of JAMSTEC to extend the coverage of heat flow data outside the active hydrothermal site. During the NT07-11 and NT07-13 cruises in 2007, *Hyper Dolphin* was used to perform heat flow measurements in the eastern area of the active hydrothermal site. During the KY08-01 cruise in 2008, we obtained sediment cores and heat flow data around the Iheya-North knoll complex in order to compare heat flow data within and outside of the Iheya-North hydrothermal field. Sediment samples collected during the KY08-01 and the KY05-14 cruises were used for measurements of thermal conductivity.

Single-channel seismic reflection profiles were collected along 26 lines during the YK06-09 cruise, forming a dense orthogonal grid. A multi-channel seismic survey was carried out during the KY07-03 cruise. During the YK07-07 cruise, the Autonomous Underwater Vehicle (AUV) *Urashima* of JAMSTEC was used to acquire high-resolution bathymetry with a multi-narrow beam echo sounder and seafloor images with a side-scan sonar. In this paper, bathymetry data and one single-channel seismic profile are used to help interpreting heat flow data.

Heat flow value is calculated as the product of geothermal gradient and thermal conductivity. In this study, we used two types of heat flow probes. A stand-alone heat flow (SAHF) meter is designed to measure the temperature gradient from a submersible or ROV (Kinoshita, 2006b). Five thermistors are mounted in the probe at 11-12 cm intervals; the probe length is 60 cm. For operation from research vessels or NSS, 4-m-long geothermal probes are used (Kinoshita et al.,

2006a). Six to eight thermistors are attached to a steel rod or a piston core sampler, and the probe is lowered from the ship to the seafloor by a steel wire.

Thermal conductivity was measured from core samples, using a half-space or needle probe method (Von Herzen and Maxwell, 1959). In the case that core samples were unavailable, the conductivity was substituted with values measured at the nearest station or with those determined for a similar lithology. The value of thermal conductivity for marine sediments varies between 0.8 and 1.2 Wm<sup>-1</sup>K<sup>-1</sup>, corresponding to the range in porosity (60%-80%). Given that thermal conductivity could not be obtained in the active site, we assumed the value of ~1 Wm<sup>-1</sup>K<sup>-1</sup>, similar to those for marine surface sediments. It may underestimate the heat flow in this area because sulfide minerals have higher conductivity. However, since preliminary inspection of core samples indicates that the surface sediment is primarily consists of altered clay or pumice, its uncertainties would be smaller than a factor of 2, which does not affect the overall heat flow trend discussed here.

To determine the geothermal gradient, sub-bottom temperatures were measured by a probe with multiple thermistors for 10-15 minutes after penetration into sediment. The effect of frictional heating was numerically removed from measured values to estimate *in situ* temperature (Bullard, 1954). The thermal gradient was corrected for the probe tilt angle, as measured either inside the probe or estimated from video images during submersible operations.

The thermistor measures electrical resistance, which is converted to temperature with 1-mK resolution. Each thermistor is calibrated from 0 to 20 °C using a quartz thermometer and an isothermal bath with an accuracy of ~10 mK. The overall absolute accuracy of the employed thermistors is estimated to be 10-20 mK. In the deep-sea environment deeper than ~200 m, bottom-water temperature is considered to be stable within several milli Kelvin. Thus, to obtain a more accurate temperature gradient, temperature is measured above the seafloor before penetration, and is subtracted from the in situ temperature. As a result, we gain a relative temperature precision in the order of milli Kelvin. Frictional heating or physical movement of the probe during measurement introduces errors to the calculated temperature gradient. Where identified, measurements containing such errors were excluded from the data.

Variations in bottom-water temperature result in nonlinear temperature-depth profiles. The degree of

nonlinearity depends on the amplitude and period of variation, as well as the thermal diffusivity of the sediment. Such variations have a negative effect on the quality of heat flow values. For example, warm water mass emitted from a vent causes an increase in sub-bottom temperatures and a decrease in the apparent temperature gradient. We estimate that the overall accuracy of the measured temperature gradient is  $\sim 10$ %, which is mainly attributed to uncertainty in thermal conductivity.

### 3. Heat Flow Distribution

We obtained 78 reliable heat flow values in and around the Iheya-North hydrothermal field. Fig. 3(a-f) shows temperature-depth profiles, and Figs. 3g and 3h, are thermal conductivity-depth profiles. Table 1 shows the result of heat flow. Thermal conductivities measured for core samples are 1.0 Wm<sup>-1</sup>K<sup>-1</sup> outside the knoll complex and 1.12 Wm<sup>-1</sup>K<sup>-1</sup> obtained in basins within the knoll complex.

## 3.1. Area around the active hydrothermal site

As shown in Fig. 2, extremely high and widely scattered heat flow values (0.1-100 Wm<sup>-2</sup>) were obtained within ~500 m of the active hydrothermal site (purple region in Fig. 1c). We designate this area a "high-heat-flow zone". Maximum heat flow values (10-100 Wm<sup>-2</sup>) were measured close to some of the mounds in the active hydrothermal site (Fig, 2). Some of them are thermally affected by the nearby venting or diffuse hydrothermal discharge, as indicated by convex temperaturedepth profiles (D218-SHF6 in Fig. 3). Note that we define 'convex' profile so that the depth which gives a certain temperature value is always shallower than the expected linear trend, whereas for the 'concave' profile its depth is always deeper. The region with heat flow ranging 1 to 10 Wm<sup>-2</sup> surrounds the active hydrothermal site. In the southwestern edge of the active site, heat flow obtained at NT03-09 D218-SHF2 is very low (< 0.1 Wm<sup>-2</sup>), and the temperature-depth profile has a concave shape (Fig. 3a; Table 1).

Beyond 500 m from the active hydrothermal site in the high-heat-flow zone, heat flow is between 0.1 and 1.0  $Wm^{-2}$ , showing a gradual eastward decreasing trend (Fig. 1(d)). All of the temperature-depth profiles obtained for this area are linear, indicating conductive heat transfer. We designate this area a "moderate-heat-flow zone".

At 1.5-2 km east of the active hydrothermal site, heat

flow values are very low (<0.1 Wm<sup>-2</sup>; e.g., YK06-09 D693-SHF105). Temperature-depth profiles in this area are nonlinear, making it difficult to obtain accurate estimates of the heat flow, although the upper bound can be estimated to be lower than 0.1 Wm<sup>-2</sup>. These nonlinear profiles are attributed to variations in bottom-water temperature. We designate this area a "low-heat-flow zone".

We should notice that heat flow values are affected by local topographic highs or lows. Surface heat flow is reduced by up to 10 % if measurements are made near the foot of a knoll in the Iheya-North field, assuming the isothermal surface. Rapid sedimentation, such as volcanic debris flow or landslides, would homogenize the temperature near the seafloor, making surface heat flow significantly low. Rugged topography in the low-heat-flow zone may support the occurrence of such events. However, cover sediment for one event, which would be less than a few meters thick, will be thermally equilibrated after one month. Thus we exclude this possibility here.

#### 3.2. Area outside of the knoll complex

Six heat flow measurements were obtained on the trough floor in an area located outside the Iheya-North knoll complex, 5-15 km from the hydrothermal field (Fig. 1(b)). Core samples from these sites consist primarily of hemipelagic clay and layers of fine-grained sand. The temperature gradient was measured at the time of coring. The obtained heat flow values are 0.07-0.17 Wm $^2$ , with an average of  $0.12\pm0.08$  Wm $^2$ . The heat flow values are consistent with those reported previously from the middle Okinawa Trough (Kinoshita and Yamano, 1997). Thus, we use this value as a "reference" value in the present analysis, because these values are not affected by the hydrothermal circulation in the Iheya-North knoll complex.

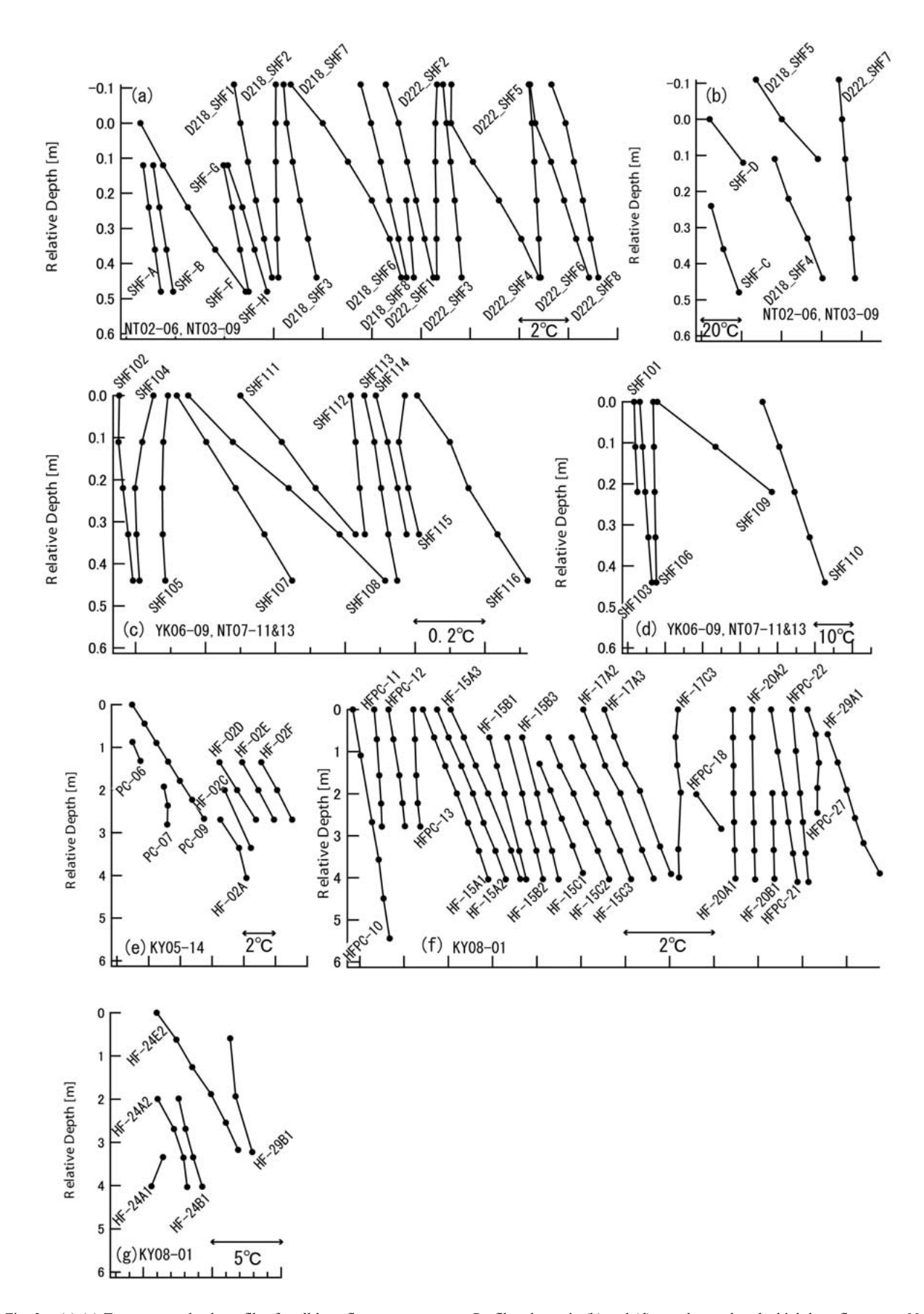


Fig. 3. (a)-(g) Temperature-depth profiles for all heat flow measurements. Profiles shown in (b) and (d) are observed at the high-heat-flow zone. Note that the scales are different from (a), (c), and (e)-(g).

Table 1. Summary of heat flow measurements

Cruise#	Station	Latitude(N)	Longitude(E)	WD m	N	Pen m	G Km <sup>-1</sup>	$\begin{array}{c} K \\ W \ m^{\text{-}1} K^{\text{-}1} \end{array}$	Qc W m <sup>-2</sup>	Comments
NT02-06	D1348-SHF-A	27° 47.413'	126° 54.109'	1040	4	0.4	2	1.03	2.1	Linear profile
T02-06	D1342-SHF-B	27 47.397	126 54.02	1050	4	0.4	2.3	1.03	2.4	Linear profile
T02-06	D1342-SHF-C	27 47.404	126 53.96	1052	3	0.3	66	1.03	68	Linear profile. Max. temp ~ 18 degC
T02-06	D1342-SHF-D	27 47.389	126 53.856	1030	2	0.2	(140)	1.03	(144)	Only 2 sensors in the mud Max. temp ~ 25 degC
T02-06	D1343-SHF-F	27 47.361	126 53.811	1017	5	0.5	9.7	1.03	10	Linear profile, measured for 1 day
T02-06	D1348-SHF-G	27 47.362	126 53.745	996	4	0.4	2.8	1.03	2.9	Linear profile
T02-06	D1348-SHF-H	27 47.385	126 53.674	983	4	0.4	4.2	1.03	4.3	Linear profile
Г03-09	D218-SHF1	27 47.296	126 53.829	1004	5		2.9	1.03	3	Linear, excellent profile
Г03-09	D218-SHF2	27 47.341	126 53.804	1017	5		0.26	-	0.06*	Concave profile
Γ03-09	D218-SHF3	27 47.362	126 53.795	1018	5		2.9	-	2.2*	Concave profile
Г03-09	D218-SHF4	27 47.398	126 53.797	1015	4		74	1.03	76	Max. temp.~28 degC
Г03-09	D218-SHF5	27 47.474	126 53.788	1001	2		160	1.03	(165)	Max. temp. >> 32 degC
Г03-09	D218-SHF6	27 47.551	126 53.78	993	5		6.2	-	11*	Convex profile
Г03-09	D218-SHF7	27 47.602	126 53.775	986	5		3.3	1.03	3.4	Linear, excellent profile
Γ03-09	D218-SHF8LT	27 47.656	126 53.779	1002	4		1.1	1.03	1.1	Measured for 7 days
Γ03-09	D222-SHF1	27 47.537	126 53.89	1033	5		3.2	1.03	3.3	Linear, excellent profile
Г03-09	D222-SHF2	27 47.659	126 53.933	1038	5		0.16	1.12	0.18	Bottom-water temperature variation
Γ03-09	D222-SHF3	27 47.55	126 53.997	1055	5		1.4	1.12	1.6	Linear, excellent profile
Γ03-09	D222-SHF4	27 47.286	126 53.993	995	5		7.1	1.03	7.3	Linear, excellent profile
Γ03-09	D222-SHF5	27 47.277	126 53.758	1005	5		0.78	1.03	0.8	Linear, excellent profile
Γ03-09	D222-SHF6	27 47.416	126 53.663	994	5		4.7	1.03	4.8	Linear, excellent profile
Г03-09	D222-SHF7	27 47.493	126 53.662	982	5		14.9	1.03	15.4	Linear, excellent profile
Γ03-09	D222-SHF8	27 47.663	126 53.69	987	5		3	1.03	3.1	Linear, excellent profile
Y05-14	PC-06	27 47.4	126 54.27	1030	2	2	(1.1)	1.19	(1.31)	Sensor string was cut off at penetration
Y05-14	PC-07	27 47.31	126 54	950	3	2.7	7.6	1.03	7.8	Linear gradient for upper 1 m, isothermal (12 degC) below
Y05-14	PC-09	27 47.61	126 54.2	1068	7	2.7	1.7	1.12	1.9	Linear, excellent profile
Y05-14	HF-02A	27 47.554	126 54.014	1055	3	2.7	1.1	1.12	1.2	Linear profile
Y05-14	HF-02B	27 47.546	126 54.038	1055	-	fell	-	-	-	Probe failed to penetrate
Y05-14	HF-02C	27 47.47	126 54.038	1055	2	1.5	1.2	1.12	(1.3)	Only 2 sensors in the mud
Y05-14	HF-02D	27 47.549	126 54.069	1055	3	2	1.7	1.12	1.9	Linear profile
Y05-14	HF-02E	27 47.557	126 54.087	1055	3	2	1.5	1.12	1.7	Linear profile
Y05-14	HF-02F	27 47.562	126 54.142	1055	3	2	1.5	1.12	1.7	Linear profile
K06-09	D962-SHF101	27 47.465	126 53.923	1045	3		5.5	1.03	5.7	partial penetration due to hard layer Max. temp.~22 degC
<b>C</b> 06-09	D962-SHF102	27 48.023	126 55.212	1013	5		0.086	1.03	0.09	
X06-09	D963-SHF103	27 47.583	126 53.962	1028	5		7.4	1.03	7.6	
K06-09	D963-SHF104	27 47.548	126 54.778	1143	5		-0.02	1.03	(-0.015)	Bottom-water temperature variation
<b>C</b> 06-09	D963-SHF105	27 47.508	126 54.946	1097	5		0.02	1.03	0.021	
<b>ζ</b> 06-09	D964-SHF106	27 47.969	126 53.763	1038	5		2.06	1.03	2.1	
X06-09	D965-SHF107	27 47.253	126 53.768	1003	5		0.76	1.03	0.78	
X06-09	D965-SHF108	27 47.403	126 54.11	1048	5		1.25	1.03	1.3	
Γ07-11	D696-SHF109	27 47.397	126 53.863	1065	3		139	1.03	143	
Γ07-11	D696-SHF110	27 47.351	126 53.655	1018	5		37.54	1.03	39	
Γ07-11	D696-SHF111	27 47.666	126 53.507	965.3	4		0.97	1.07	1	
Γ07-13	D712-SHF112	27 47.684	126 54.045	1022	5		0.14	1.12	0.16	
Γ07-13	D712-SHF113	27 47.678	126 54.125	1044	5		0.2	1.12	0.22	
Γ07-13	D713-SHF114	27 47.39	126 54.599	1060	4		0.25	1.03	0.26	
Γ07-13	D713-SHF115	27 47.399	126 54.750	1079	5		0.18	1.03	0.19	
Γ07-13	D713-SHF116	27 47.392	126 54.892	1114	4		0.76	1.03	0.78	
Y08-01	HFPC-10	27 47.442	126 46.333	1451	5	8	0.155	1.09	0.17	
	HFPC-11	27 45.857	126 50.793	1488	6	3.28	0.068	1.02	0.07	
	HFPC-12	27 49.659	126 58.504	1263	5	4.43	0.134	1	0.13	
	HFPC-13	27 46.305	126 58.509	1278	5	-	0.057	1.07	0.06	
Y08-01	HFPC-14	27 49.010	126 54.809	1263	-	-	-	-	-	

Cruise#	Station	Latitude(N)	Longitude(E)		N	Pen	G Vm <sup>-1</sup>	K W m-1V-1	Qc W m-2	Comments
				m		m	Km <sup>-1</sup>	W m <sup>-1</sup> K <sup>-1</sup>	W m <sup>-2</sup>	
CY08-01	HF-15A1	27 47.401	126 54.349	1030		4.31	0.4	1.19	0.48	
Y08-01	HF-15A2	27 47.401	126 54.349	1034		4.68	0.37	1.17*	0.43	
Y08-01	HF-15A3	27 47.405	126 54.351	1037	6	4.73	0.39	1.2*	0.47	
Y08-01	HF-15B1	27 47.397	126 54.435	1056	4	4.31	0.25	1.08	0.27	
Y08-01	HF-15B2	27 47.397	126 54.440	1053	5	4.31	0.24	1.06*	0.25	
Y08-01	HF-15B3	27 47.397	126 54.437	1052	5	4.31	0.24	1.1*	0.26	
Y08-01	HF-15C1	27 47.401	126 54.515	1062	5	4.31	0.38	1.09*	0.41	
Y08-01	HF-15C2	27 47.402	126 54.516	1059	6	4.31	0.41	1.11*	0.46	
Y08-01	HF-15C3	27 47.402	126 54.517	1062	6	4.31	0.41	1.11*	0.46	
Y08-01	HF-17A1	27 47.451	126 54.647	1076	-	fell	-	-	-	
Y08-01	HF-17A2	27 47.453	126 54.648	1078	6	4.31	0.4	1.03	0.41	Linear, excellent profile
Y08-01	HF-17A3	27 47.449	126 54.649	1076	6	4.61	0.4	1.03	0.41	Linear, excellent profile
Y08-01	HF-17B1	27 47.526	126 54.759	1130	-	fell	-	-	-	
Y08-01	HF-17B2	27 47.533	126 54.759	1128	-	fell	-	-	-	
Y08-01	HF-17B3	27 47.530	126 54.760	1129	-	fell	-	-	-	
Y08-01	HF-17C1	27 47.558	126 54.758	1133	-	fell	-	-	-	
Y08-01	HF-17C2	27 47.567	126 54.764	1133	-	fell	-	-	-	
Y08-01	HF-17C3	27 47.563	126 54.763	1131	6	4	0.02	1.03	(0.21)	Bottom-water temperature variation
Y08-01	HFPC-18	27 46.097	126 54.905	780	2	1.3	0.69	1.07	(0.74)	Only 2 sensors in the mud
Y08-01	HF-20A1	27 48.213	126 55.108	1162	7	4.3	0.014	1.03	0.014	
Y08-01	HF-20A2	27 48.208	126 55.117	1106	6	4.3	0.016	1.03	0.016	
Y08-01	HF-20B1	27 48.173	126 55.103	1095		2.5	0.02	1.03	0.021	Linear profile
Y08-01	HFPC-21	27 44.523	126 55.274	1477	5	6.5	0.14	0.99	0.14	Linear, excellent profile
Y08-01	HFPC-22	27 48.013	126 58.001	1279	5	6	0.089	1	0.09	Linear, excellent profile
Y08-01	HFPC-23	27 46.395	126 57.379	730		2	_	_	(<0.1)	Bottom-water temperature variation
Y08-01	HF-24A1	27 47.603	126 53.848	942	2	4	10.98	1.12	12	Linear gradient for upper 1.5 m, isothermal (~26 degC) below
Y08-01	HF-24A2	27 47.603	126 53.857	948	4	2.5	17.2	1.12	19	Linear gradient for upper 0.5 m, low grdient (~17 degC) below
Y08-01	HF-24B1	27 47.652	126 53.869	957	5	3	0.8	1.12	0.9	Linear profile
Y08-01	HF-24C1	27 47.708	126 53.840	950		fell	_	_	-	•
Y08-01	HF-24C2	27 47.705	126 53.844	949		fell	_	_	-	
Y08-01	HF-24C3	27 47.723	126 53.849	947		fell	_	_	_	
Y08-01	HF-24D1	27 47.769	126 53.852	960		fell	_	_	_	
Y08-01	HF-24D2	27 47.776	126 53.859	963		fell	_	_	-	
Y08-01	HF-24D3	27 47.777	126 53.859	970		fell	_	-	-	
Y08-01	HF-24D4	27 47.778	126 53.858	967		fell	_	_	-	
Y08-01	HF-24E1	27 47.807	126 53.880	987		fell	_	_	-	
Y08-01	HF-24E2	27 47.816	126 53.881	981		4.4	2.09	1.03	2.2	
Y08-01		27 47.002	126 53.826	1079		1.5	0.098	1.03	(0.1)	Only 2 sensors in the mud
Y08-01		27 47.701	126 53.502	926	2	1.3	2.61	1.07	(2.8)	Only 2 sensors in the mud
Y08-01	HFPC-27	27 47.588	126 54.849	1135		2.8	0.035		(0.036)	Bottom-water temperature variation
Y08-01	HFGC-28	27 47.493	126 53.744		-	fell	-	-	-	Too hard to penetrate
Y08-01		27 47.554	126 54.566	1040		4.16	0.3	1.03	0.31	Linear profile
Y08-01		27 47.585	126 54.648	1042		>4	0.29	1.03	0.3	Concave?
Y08-01	HF-29C1	27 47.565	126 54.688	1065		fell	0.27	1.03	-	Consure.
Y08-01	HF-29C1	27 47.568	126 54.692	1058		fell	_	_	_	
. 1 00-01	111-2702	2/ 7/.500	120 27.072	1050	-	1011	-	-	-	

# Notes:

WD: the Water depth, N: the number of sensors used for calculation of temperature gradient, Pen: the penetration length of the probe, G: the temperature gradient, K: the thermal conductivity (\*indicates data estimated by the insitu heat-pulse method), Q: the conductive heat flow (\* is the total heat flow estimated from nonlinear temperature profiles, assuming they result from both conductive and advective heat transfer, after Bredehoeft and Papadopulos, 1965).

#### 4. Discussion

Fig. 5 shows a single-channel seismic profile (raw and interpreted) along Line 18HD (see Fig. 1) and a cross-section of all heat flow within the knoll complex projected along this line. The high-heat-flow zone (shown in Fig. 1c) is limited to within 500 m of the active hydrothermal site, which is the primary hydrothermal discharge in the Iheya-North field. The surface at the active hydrothermal site consists of coarse-grained sediment, primarily volcanic clastics and sandy pumice. A sediment core, collected near the active site using a 4-m-long piston core sampler, shows a layered structure and contains layers dominated by massive pumice or pumice fragments (Kinoshita et al., 2006a). In this setting, the pumice-rich layers would serve as permeable channels or a potential hydrothermal reservoir.

In the low-heat-flow zone, located 1.5-2.0 km east of the active site, visual observations and side-scan sonar images suggest that the seafloor consists of coarse sediment with a rugged surface, as revealed from high-resolution bathymetry obtained using AUV Urashima (Fig. 2; Kumagai et al., 2010). Here, heat flow is much lower than the reference value (0.1 Wm $^{-2}$ , see Section 3.2). As seen in Fig. 3, temperature-depth profiles for these low heat flow stations (e.g. NT03-09 D222-SHF2, YK06-09 SHF104, KY08-01 HF-17C3) are not linear with their non-linearity of up to  $\sim$ 0.1 K. The variation of bottom-water temperature is its most likely cause (see Section 2), which can apparently change surface temperature gradient by  $\sim$ 0.1 Km $^{-1}$ . It implies that the low-heat-flow zone may have

the heat flow value similar to the reference site outside the knoll complex. Long-term heat flow monitoring is ultimately necessary, but we are not in favor of this possibility, because measurements were made in different cruises and in different probe lengths, making it difficult to produce consistently low temperature gradient only by the increase in the bottom-water temperature.

Instead, we suggest that such anomalously low heat flow is better explained by the recharge of seawater into the formation; it is likely that the high permeability beneath this zone enables the seawater to infiltrate the seafloor sediment, resulting in a reduction in surface heat flow values.

In the moderate-heat-flow zone, heat flow gradually decreases eastward, approaching the value in the low-heat-flow

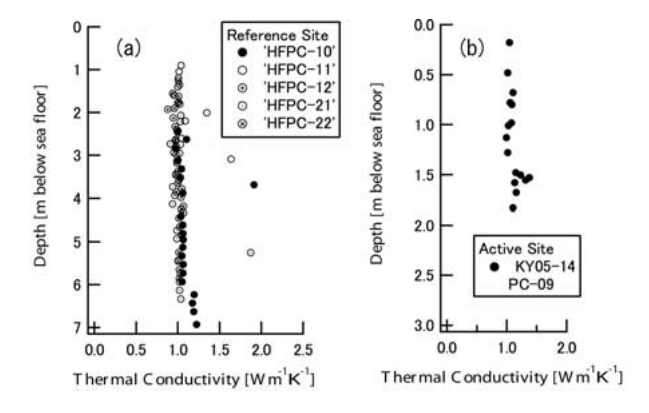


Fig. 4. (a) Thermal conductivity-depth profiles in the area outside the knoll complex, obtained during the KY08-01 cruise, (b) Thermal conductivity-depth profile in the active hydrothermal site, obtained during cruise KY05-14.

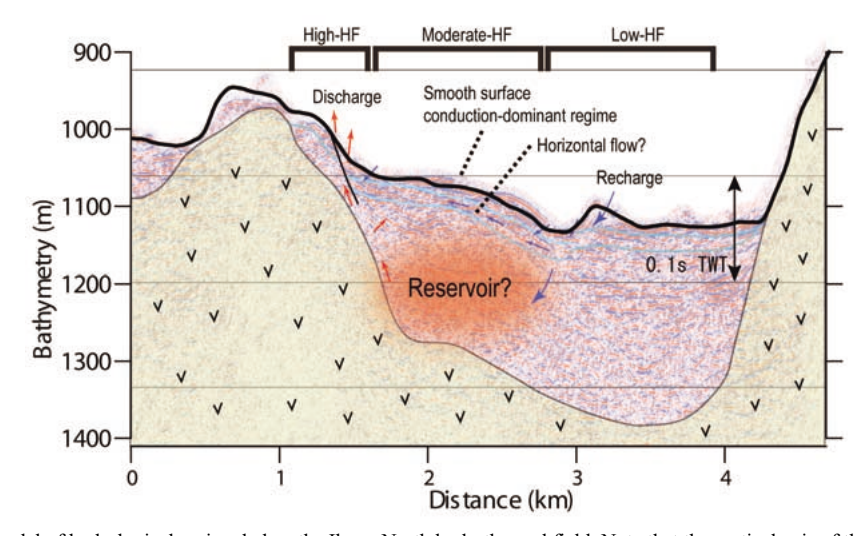


Fig. 5. Hypothetical model of hydrological regime below the Iheya-North hydrothermal field. Note that the vertical axis of the seismic profile HD18 (see Fig. 1 for location) is a two-way travel time (TWT). Single-channel seismic line HD18 was obtained during cruise YK06-09. 'High-HF' stands for high-heat-flow zone.

zone, but values are still higher than the reference value outside the knoll complex. Seafloor observation revealed a distinctive change in surface lithology from coarse-grained sediment in the active hydrothermal site to smooth clay-rich sediment (Oiwane et al., 2008) at a site located several hundred meters to the east.

The seismic profile reveals several horizons below the moderate-heat-flow zone; however it is not clear whether these reflectors continue to the east or west. Based on descriptions of a piston core sample recovered from this zone, the horizontally stratified sub-surface structure may indicate intercalated layers of clayey, sandy, and pumice-rich sediments. Such a structure would have a strong vertical anisotropy in permeability, suppressing vertical fluid flow and resulting in a vertically conductive thermal regime near the seafloor.

The above results represent a qualitative model of horizontally elongated hydrothermal circulation within the Iheya-North knoll complex, with a horizontal scale of 2-3 km and vertical scale of less than 1 km, where the horizontal fluid flow occurs from the region below the low-heat-flow zone toward the hydrothermal reservoir located below the high-heat-flow zone. We infer that hydrothermal vents or diffuse flow can drive this circulation if the sediment below the moderate-heat-flow zone is impermeable enough to prevent vertical fluid migration but is permeable enough to encourage flow in the lateral direction. In the Iheya-North system, the seafloor and sub-bottom horizons are actually inclined toward the high-heat-flow zone. This slope is as large as 10 % below the moderate-heat-flow zone, which should also encourage the fluid flow.

A similar circulation system has been proposed by Genthon et al. (1990) for another basin in the Okinawa Trough, where the sedimentary layer is ~2 km thick and the heat flow across the basin varies from 32 to 232 Wm<sup>-2</sup> over a distance of 30 km. The authors reported that horizontal permeability is greater than vertical permeability by a factor of >100, resulting in large-scale hydrothermal circulation.

We believe that a significant amount of heat exchange occurs through the kilometer-scale hydrothermal circulation that we propose in this paper. A larger scale circulation is proposed where the fluid is supplied from outside of the knoll complex, based on a calculation of methane balance between hydrothermal fluid output and the source carbon supply, and based on the sediment-derived chemical signatures in hydrothermal fluids (Kawagucci et al., 2010). The methane mass and isotopic balance in the Iheya-North hydrothermal fluids strongly suggest that almost all of the hydrothermal source would be derived from the pore fluid in the sediments

filling the mid-Okinawa Trough around the Iheya-North knoll.

These models require further testing through more direct measurements such as physical and hydrological properties or geochemical anomalies. Geochemical or geophysical data through drilling should significantly increase knowledge about the scale of Iheya-North hydrothermal circulation. Analysis from numerical study should also improve understanding the system.

#### 5. Conclusion

Three distinct zones with heat flows of different magnitudes-high (>1 Wm<sup>-2</sup>), moderate (0.1-1.0 Wm<sup>-2</sup>), and low (<0.1 Wm<sup>-2</sup>) - were identified within 3 km of the active site of the Iheya-North hydrothermal field in the middle Okinawa Trough. The zones of low and high heat flow are separated by ~2 km. Although we have no direct evidence yet, such heat flow distribution suggests a qualitative model of horizontally elongated hydrothermal circulation within the Iheya-North knoll complex, with a horizontal scale of 2-3 km and vertical scale of less than 1 km, where the horizontal fluid flow occurs from the region below the low-heat-flow zone toward the hydrothermal reservoir located below the high-heat-flow zone. This model needs to be tested through other, more direct evidence and by numerical simulation studies.

# Acknowledgements

We are grateful to the officers and crew of JAMSTEC research vessels for outstanding professionalism and dedication that made the cruises a success. We thank the scientific parties for collaboration and discussion. We are indebted to marine technicians from Nippon Marine Enterprises and Marine Works Japan for their invaluable help at sea. Discussions with H. Oiwane, H. Kumagai, M. Asada, T. Tsuji, and T. Fujiwara proved invaluable in preparing the manuscript. Comments by two referees were helpful in improving the manuscript. This work is a contribution of the research program at IFREE JAMSTEC and a joint program between Kochi University and JAMSTEC.

# References

- Auzende, J.M., E. Honza, X. Boespflug, S. Deo, J. P. Eissen, J. Hashimoto, P. Huchon, J. Ishibashi, Y. Iwabuchi, P. Jarvis, M. Joshima, K. Kishimoto, Y. Kuwahara, Y. Lafoy, T. Matsumoto, J. P. Maze, K. Mitsuzawa, H. Monma, T. Naganuma, Y. Nojiri, S. Ohta, K. otsuka, Y. Okuda, H. Ondreas, A. Otsuki, E. Ruellan, M. Sibuet, M. Tanahashi, T. Tanaka, and T. Urabe, Active spreading and hydrotherrmalism in North Fiji Basin (SW Pacific) (1990), Results of Japanese French Cruise Kaiyo 87, *Mar. Geophys. Res.*, 12, 269-283.
- Both, R., K. Crook, B. Taylor, S. Brogan, B. Chappell, E. Frankel, L. Liu, J. Sinton, and D. Tiffin (1986), Hydrothermal chimneys and associated fauna in the Manus back-arc basin, Papua New Guinea, *Eos Trans. AGU*, *67*, 489-490.
- Bredehoeft, J.D., and I.S. Papadopulos (1965), Rates of vertical groundwater movement estimated from the earth's thermal profile, *Water Resour. Res.*, 2, 325-328.
- Bullard, E. C. (1954), The flow of heat through the floor of the Atlantic Ocean, *Proc. R. Soc. London. Ser. A*, 222 (1150), 408-429.
- Craig, H., Y. Horibe, K.A. Farley, J.A. Welhan, K.R. Kim, and R.N. Hey (1987), Hydrothermal vents in the Mariana Trough, Results of the first Alvin dives, *Eos Trans. AGU*, 68, 1531.
- Genthon, P., M. Rabinowicz, J.P. Foucher, and J.C. Sibuet (1990), Hydrothermal circulation in an anisotropic sedimentary basin: application to the Okinawa back arc basin, *J. Geophys. Res.*, *95*, 19175-19184.
- Halbach, P., et al. (1989), Probable modern analogue of Kuroko-type massive sulfide deposits in the Okinawa Trough back-arc basin, *Nature*, *338*, 496-499.
- Kataoka, S., J. Ishibashi, T. Yamanaka, and H. Chiba (2000), Topography and fluid geochemistry of the Iheya North Knoll seafloor hydrothermal system in the Okinawa Trough, JAMSTEC J. Deep Sea Res, II. Geology, Geochemistry, Geophysics and Dive Survey., 16, 1-7.
- Katsura, T., S. Oshima, T. Ogino, K. Ikeda, M. Nagano, M. Uchida, M. Hayashida, K. Koyama, and S. Kasuga (1986), Geological and geophysical characteristics of the southwestern Okinawa trough and adjacent area, Report of Hydrographic and Oceanographic Researches, 21, 21-47.
- Kawagucci, S., H. Chiba, J. Ishibashi, T. Yamanaka, T. Toki,

- Y. Muramatsu, Y. Ueno, A. Makabe, K. Inoue, N. Yoshida, S. Nakagawa, T. Nunoura, K. Takai, N. Takahata, Y. Sano, T. Narita, G. Teranishi, H. Obata, and T. Gamo, Hydrothermal fluid geochemistry at the Iheya North field in the mid-Okinawa Trough: Implication for origin of methane in subseafloor fluid circulation systems, *Geochemical Journal*, accepted.
- Kimura, M., Y. Kato, T. Tanaka, J. Naka, T. Gamou, M. Yamano, M. Ando, S. Uyeda, H. Sakai, T. Oomori, E. Izawa, M. Kanenaga, T. Ono, and A. Oshida (1987), Submersible *Shinkai2000* study on the central rift in the middle Okinawa trough, *JAMSTECTR Deepsea Research*, 3, 165-196.
- Kinoshita, M., M. Yamano, Y. Kasumi, and H. Baba (1991), Report on DELP 1988 cruises in the Okinawa Trough Part 8: Heat flow measurements, *Bulletin of the Earthquake Research Institute University of Tokyo*, 66, 211-228.
- Kinoshita, M (1995), Localized heat flow anomalies in the middle Okinawa Trough associated with hydrothermal circulation, in Biogeochemical Processes and Ocean Flux in the Western Pacific, edited by H. Sakai and Y. Nozaki, 537-599 pp., Terra Scientific Publishing Company (TERRAPUB).
- Kinoshita, M. and M. Yamano (1997), Hydrothermal regime and constraints on reservoir depth of the Jade site in the Mid-Okinawa Trough inferred from heat flow measurements, *J. Geophys. Res.*, 102, 3183-3194.
- Kinoshita, M., T. Nunoura, J. Ashi, and KY05-14 cruise Shipboard Scientific Party (2006a), Hydrothermal regime of Iheya-North hydrothermal field, Mid-Okinawa Trough, inferred from heat flow and samples obtained using NSS, Japan Geoscience Union, abstract J161-P016.
- Kinoshita, M., Y. Kawada, A. Tanaka, and T. Urabe (2006b), Recharge/discharge interface in the Suiyo Seamount hydrothermal system detected by submersible-operated heat flow measurements, *Earth and Planetary Science Letters*, 245, 498-508.
- Kinoshita, M., M. Yamano, J. Post, and P. Halbach (1990), Heat flow measurements in the southern and middle Okinawa Trough on R/V Sonne in 1988, *Bulletin of the Earthquake Research Institute University of Tokyo*, 65, 571-588.
- Kumagai, H., S. Tsukioka, H. Yamamoto, T. Tsuji, K. Shitashima, M. Asada, F. Yamamoto, and M. Kinoshita

- (2010), Hydrothermal plumes imaged by high-resolution side-scan sonar on a cruising AUV, Urashima, *Geochem. Geophys. Geosyst., 11 (12)*, Q12013, doi:10.1029/2010GC003337
- Lees, C.H. (1910), On the shapes of the isogeotherms under mountain ranges in radio-active districts. *Proceedings of the Royal Society of London. Ser. A, 83*, 339-46.
- Momma, H., R. Iwase, K. Mitsuzawa, Y. Kaiho, Y. Fujiwara, Y. Amitani, and M. Aoki (1996), Deep Tow Survey in Nanseishoto Region (K95-07-NSS), *JAMSTEC J. Deep Sea Res.*, 12, 195-210.
- Nagumo, S., H. Kinoshita, J. Kasahara, T. Ouchi, H. Tokuyama, S. Koresawa, and H. Akiyoshi (1986), Report on 1984 DELP cruise in the middle Okinawa Trough, Part II: Seismic structural studies, *Bull. Earthquake Res. Inst.*, 61, 167-202.
- Oiwane, H., H. Kumagai, Y. Masaki, H. Tokuyama, M. Kinoshita KY08-01 Shipboard Science Party, and M. Kinoshita (2008), Characteristics of Sediment in Iheya North Knoll and 'the acoustic blanking layer', *JPGU*, J164-013.
- Sibuet, J.-C., J. Letouzey, F. Barbier, J. Charvet, J.-P. Foucher, T.C. Hilde, M. Kimura, C. Ling-yun, B. Marsset, C. Mullar, and J.-F. Stephan (1987), Back arc extension in the Okinawa Trough, *J. Geophys. Res.*, 92, 14041-14063.
- Von Herzen, R.P. and A.E. Maxwell (1959), The measurement of thermal conductivity of deep-sea sediments by a needle-probe method, *J. Geophys. Res.*, 64, 1557-1563.
- Yamano, M., S. Uyeda, H. Kinoshita, and T.W.C. Hilde (1986a), Report on DELP 1984 Cruise in the Middle Okinawa Trough Part IV: Heat Flow Measurements, Bulletin of the Earthquake Research Institute University of Tokyo, 61, 251-267.
- Yamano, M., S. Uyeda, Y. Furukawa, and G.A. Dehghani (1986b), Heat flow measurements in the northern and middle Ryukyu Arc area on R/V SONNE in 1984, Bulletin of the Earthquake Research Institute University of Tokyo, 61, 311-327.
- Yamano, M., S. Uyeda, and M. Kinoshita (1988), Heat flow and hydrothermal circulation in the middle Okinawa Trough, *Chikyukagaku (Geochemistry)*, 22, 57-64.